Original Article

Artificial High- and Low-density Materials in Bone Mineral Densitometry Using Dual-energy X-ray Absorptiometry: A GATE Monte Carlo Simulation of "Black-hole" Artifact

Mohsen Qutbi

Department of Nuclear Medicine, School of Medicine, Shahid Beheshti University of Medical Sciences, Tehran, Iran

Abstract

Objective: The objective of the study was to evaluate the effect of artificial high- and low-density materials on Bone mineral density (BMD) scans in dual-energy X-ray absorptiometry (DXA) method and emergence of black-hole artifact through GATE Monte Carlo simulation. **Materials and Methods:** GATE Monte Carlo code was utilized to simulate the artifact encountered in clinical scans acquired by HOLOGIC® bone densitometer. Two simplified phantoms were designed. The first one was a rectangular box with six smaller cubes inside and the second one was a body torso. Materials of cubes were spine bone, polymethyl methacrylate (PMMA), barium sulfate suspension in water, stainless steel, titanium alloy, and gold. The torso phantom contained objects of 5 vertebrae, bowel and 3 small spherical objects near the surface of the torso as piercing objects on the abdominal wall, each overlying the vertebrae. Using 100 and 140 kVp, spectral X-rays were generated to simulate DXA. For both phantoms, two simulations were carried out. The pair of projections acquired for each phantom were then subtracted and analyzed by curve fitting techniques. **Results:** Except for spine bone, in which radio-opacity decreases with increasing spectral X-ray energy (from 100 to 140 kVp), other squares exhibit little changes over different energies. PMMA shows consistently very low radio-opacity. Four other materials (barium sulfate in water, stainless steel alloy, titanium alloy, and gold), all attenuate the X-ray photons substantially. Except for spine bone, other materials are barely noticeable in pairwise subtracted images. In torso phantom, piercing objects are visualized as "holes" in vertebrae. **Conclusion:** Both artificial high- and low-density materials, compared to bone, are eliminated during the subtraction of dual-energy X-ray profiles and therefore, can create black-hole artifact.

Keywords: Artificial materials, "black-hole" artifact, bone mineral densitometry, dual-energy X-ray absorptiometry, GATE Monte Carlo simulation

Received on: 25-02-2024 **Review completed on:** 06-08-2024 **Accepted on:** 06-08-2024 **Published on:** 21-09-2024

Introduction

As a crucial indicator of bone health, bone mineral density (BMD) is currently assessed and measured utilizing dual-energy X-ray absorptiometry (DXA) in bone mineral densitometry. Leading institutions conducting research on osteoporosis recommend utilizing this method as the first-choice, preferred modality. Despite the widespread endorsement of this technique, it suffers from a number of pitfalls and flaws that have been investigated by many professionals around the world.[1-5] The principal technique of DXA is employing dual-energy X-ray photons to obtain the mineral density of bony structures with higher accuracy while removing the interfering effect of overlying soft tissues. To accomplish this task, two particular values of kVp are applied to the X-ray tube to generate two distinct spectra of X-rays. The photons in the spectrum have the minimum and maximum energies of zero and the value of kVp, respectively. Moreover, characteristic X-rays may be generated and added to the spectrum depending on the target in the X-ray tube (mostly tungsten). Consequently, two distinct radiation attenuation or absorption profiles or two-dimensional projections are produced by X-rays with two different spectral energies. After

Access this article online

Quick Response Code:

Website: www.jmp.org.in

DOI: 10.4103/jmp.jmp_36_24

Address for correspondence: Dr. Mohsen Qutbi, Department of Nuclear Medicine, Taleghani Hospital, Yaman St., Velenjak, Tehran, Iran.
E-mail: mohsen.qutbi@gmail.com/mohsen.qutbi@sbmu.ac.ir

How to cite this article: Qutbi M. Artificial high- and low-density materials in bone mineral densitometry using dual-energy X-ray absorptiometry: A GATE Monte Carlo simulation of "black-hole" artifact. J Med Phys 2024;49:433-40.

appropriate normalization of images, these two projections are subtracted to eliminate the soft tissue, leaving the bone and extra-skeletal calcified structures.[6,7] These energy levels are suitable to distinguish bone from soft tissue fairly clearly.[6,7] Materials with higher density than compact bone are commonly seen in clinical images as radiopaque structures in BMD scans. In these situations, the technician decides to scan the hip of the opposite side. But for spine, those vertebrae are excluded from the analysis. However, there appear to be some errors in the measurement of densities significantly greater than those of trabecular and compact bone. High-density artificial materials, such as surgical clips, lead bullet remnants, gunshot fragments, orthopedic metallic instruments, barium-containing contrast media in the bowels, and piercing items or jewelry can be found inside or on the surface of the body on certain occasions. These artificial high-density materials attenuate the X-ray photons of the abovementioned energies to an extreme level that there would be no perceptible difference in the attenuation profiles. Consequently, these regions are eliminated during subtraction of projections, like soft-tissue components, and as a result, appear as low-density areas, a potential pitfall of DXA method. Since the region appears black when displayed in grayscale (on a black background), some authors have called this appearance a "black-hole" artifact.[8,9] This appearance was first reported by Morgan *et al*. as an incidental finding in BMD scan of a patient with a bullet in the lumbar vertebrae. Although that was radiopaque in plain abdominal X-ray, it was observed as a low-density area in BMD scan. Hence, they called it black-hole artifact. In an experiment using HOLOGIC scanner, they observed that the certain types of metallic objects such as lead bullet and tantalum surgical clips could produce such artifact.[8,9] Although not sufficiently self-descriptive, we use this terminology in this article. Another unexplored topic is the possibility of producing a similar appearance in BMD scans when low-density materials, such as polymethyl methacrylate (PMMA), are present. PMMA is used as bone cement in vertebroplasty. These materials have densities within the ranges of soft tissues. The present study aimed to evaluate the effect of artificial high- and low-density materials on BMD scans using DXA method and the emergence of black-hole artifact through simulation by GATE Monte Carlo codes. For this task, materials with a diverse range of densities that

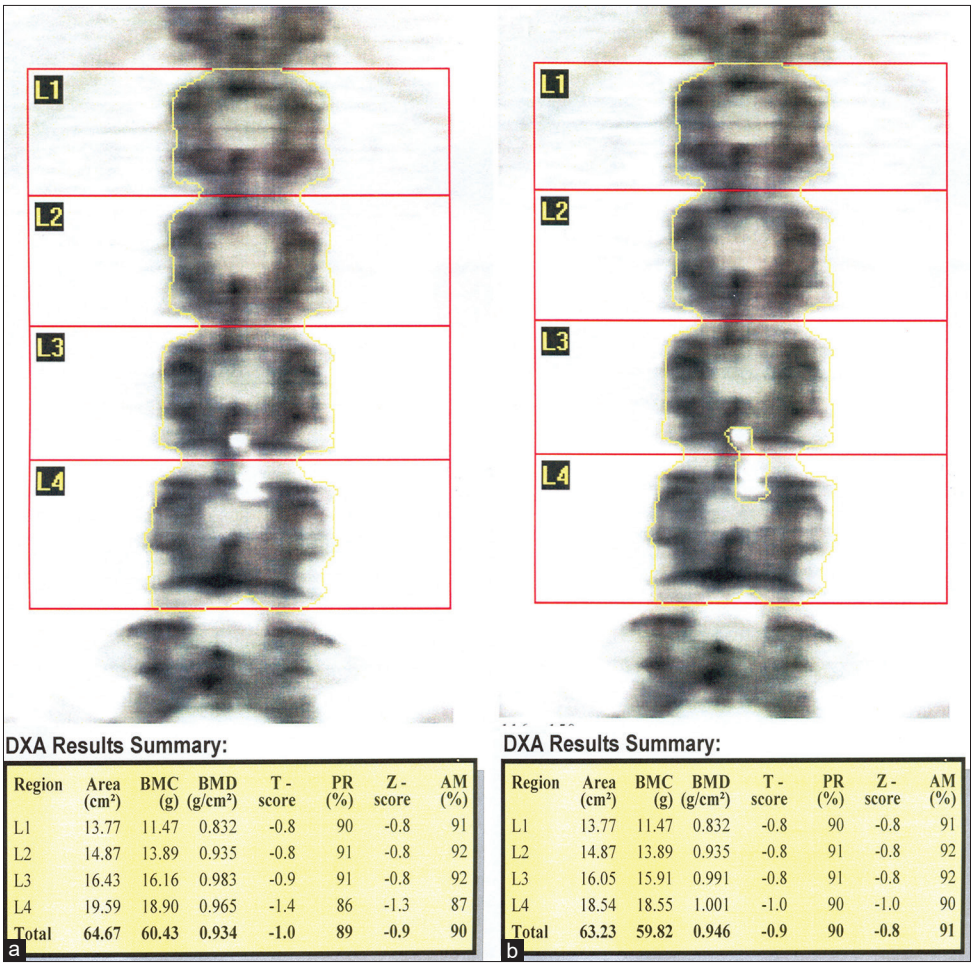

Figure 1: The results of Bone mineral density (BMD) scanning acquired by HOLOGIC® scanner are provided. In each part, the inclusion (a) Versus exclusion, (b) Of the area leads to negligible changes in the BMD and T-and Z-scores. Exclusion of this artifactual area slightly increases the areal density (g/cm^2). DXA: Dual-energy X-ray absorptiometry

may be encountered in the clinical setting were investigated: Intestinal contrast media containing barium sulfate, piercing items attached to the abdominal wall (composed of steel or titanium alloys and gold) as high-density materials, and PMMA as low-density artificial materials.

Materials and Methods

Black-hole artifact in clinical images

Herein, a case example of black-hole artifact that occurred during the BMD scan of a patient conducted by HOLOGIC® scanner is presented. A 36-year-old woman presented for bone mineral densitometry scanning. During the prescan preparation, a piece of piercing jewelry was noticed around the umbilicus. A HOLOGIC® bone densitometer (explorer QDR™ series) was used to scan the spine and hip. During the analysis of images, a small zone without detectable density was observed at the level of the third and fourth vertebrae of the lumbar spine (L3 and L4), which was excluded from the bone map of the spine. We believed it to be a "black-hole" artifact. Since this artifact generated no high-density area in BMD scan, inclusion or exclusion of that region had no noticeable impact on the final BMD result and clinical diagnosis [Figure 1].

Simulation of black-hole artifact

A GEANT4-based GATE Monte Carlo code was used to simulate and model the black-hole artifact caused by various materials during scanning by HOLOGIC® bone densitometry scanner using the method of DXA. Two simplified phantoms were created. The first one was a large rectangular box with 6 smaller cubes inside and the second phantom represents the trunk or torso of the human body. The first phantom (or rectangular cube) as seen in Figure 2a and b consists of a large box in a rectangular shape filled with water and 6 smaller cubes arranged in two rows with a 4-cm distance between adjacent edges. The dimensions of the large cube and smaller cubes are 28 cm × 19 cm × 6 cm and 4 cm × 4 cm × 4 cm, respectively. The distance between two adjacent cubes is 4 cm. The material and composition of these six cubes are as follows: spine bone (yellow), PMMA (green), barium sulfate in water (red), stainless steel (gray), titanium alloy (cyan), and gold (blue). The torso phantom is demonstrated in Figure 2c and d. The objects of vertebrae (in dark blue and white), the transverse part of the colon (magenta), and piercing objects as small spheres (stainless steel alloy in green, titanium alloy in gray, and gold in yellow) are demonstrated. The vertebra in white demonstrates the material of PMMA and the vertebrae in dark blue are made up of spine bone. The materials such as water, PMMA, and spine bone were used from the materials database embedded in the GATE Monte Carlo code and the other four materials (barium sulfate/water, stainless steel,[10] titanium alloy,[11] and gold) were constructed and added to the database. The chemical formulas of these materials are summarized in Table 1. The material was set to "Body" in the GATE materials database. Inside this geometry, 5 objects in the shape of the elliptical tube as vertebrae arranged longitudinally along the long axis of the torso (short radius = 2 cm, long radius = 3 cm, and height = 3 cm) and another cylindrical shape indicating the transverse section of colon (radius = 1 cm) were created. The latter was placed at the level of the second vertebra of the lumbar spine (L2) and was filled with barium sulfate/water. With the exception of the first vertebra (L1) which was made of PMMA, the material for other vertebrae (L2–L5) was spine bone. Three small spherical objects (radius 0.8 cm) were made near

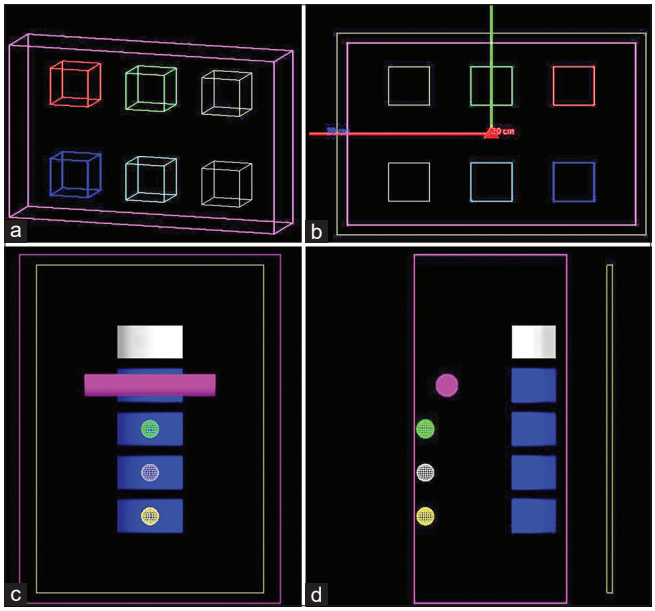

Figure 2: The geometry of the first phantom or rectangular cube (a and b) and the second phantom or body torso (c and d) Are presented. The smaller cubes (a and b) are arranged inside the larger box. The phantom of the human body torso in the front (c) and side, (d) Views are presented

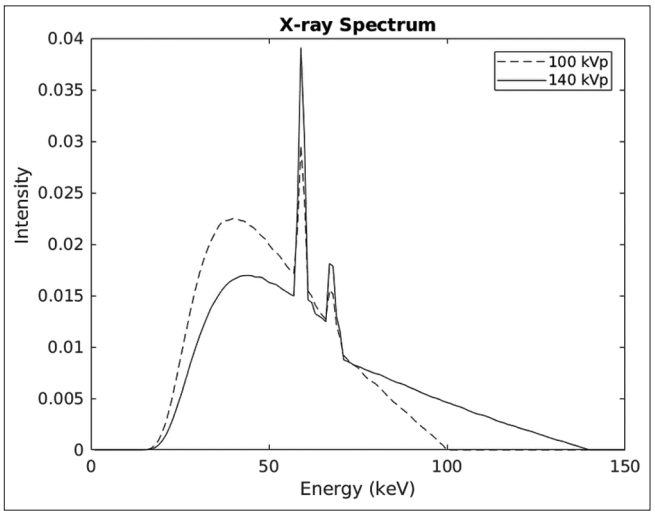

Figure 3: The spectra of X-rays generated by both 100 and 140 kVp on the X-ray tube are demonstrated. For 100 kVp, the spectrum ranges from 0 to 100 keV and for 140 kVp, the range of energy is between 0 and 140 keV. The characteristic X-rays for tungsten are displayed as sharp peaks. Because of filtration by aluminum, the parts of spectra up to 20 keV are set to zero

Table 1: Materials used for constructing phantoms in the present experiment

Materials	Label in GATE "materials" database	Elements (symbol)	Fraction (f) or *n*	Density (g/cm^3)
Water		Hydrogen (H)	*n*=2	1.00
		Oxygen (O)	*n*=1	
Body	Body	Hydrogen (H)	f=0.112	1.00
		Oxygen (O)	f=0.888	
Spine bone	Spine bone	Hydrogen (H)	f=0.063	1.42
		Carbon (C)	f=0.261	
		Nitrogen (N)	f=0.039	
		Oxygen (O)	f=0.436	
		Sodium (Na)	f=0.001	
		Magnesium (Mg)	f=0.001	
		Phosphor (P)	f=0.061	
		Sulfur (S)	f=0.003	
		Chlorine (Cl)	f=0.001	
		Potassium (K)	f=0.001	
		Calcium (Ca)	f=0.133	
Polymer of methyl-methacrylate	PMMA	Hydrogen (H)	f=0.080541	1.195
		Carbon (C)	f=0.599846	
		Oxygen (O)	f=0.319613	
Barium sulfate in water (50%)	Barium contrast*	Barium (Ba)	*n*=1	2.245
		Sulfur (S)	*n*=1	
		Oxygen (O)	*n*=4	
Stainless steel alloy	SLSteel316L*,§	Iron (Fe)	f=0.55295	8
		Chromium (Cr)	f=0.18	
		Molybdenum (Mo)	f=0.03	
		Nickel (Ni)	f=0.14	
		Nitrogen (N)	f=0.001	
		Manganese (Mn)	f=0.02	
		Silicon (Si)	f=0.075	
		Carbon (C)	f=0.0003	
		Phosphor (P)	f=0.00045	
		Sulfur (S)	f=0.0003	
Titanium alloy	TiAlloy_G5_Ti6AAl4V*,§	Titanium (Ti)	f=0.873	4.420
		Aluminum (Al)	f=0.06	
		Vanadium (V)	f=0.04	
		Iron (Fe)	f=0.025	
		Oxygen (O)	f=0.002	
Gold	Gold*	Gold (Au)	*n*=1	19.320

*Materials added by the author to the GATE materials database, §Materials as metallic alloys. PMMA: Polymethyl methacrylate

the surface of the torso as piercing objects attached to the abdominal wall, each at the level of L3–L5 vertebrae. These objects were made up of stainless steel, titanium alloy, and gold, respectively. As per the HOLOGIC® system, an X-ray gun was considered with two distinct levels of kVp. The spectrum and relative abundancy of X-ray energies that was used in this simulation was extracted from X-ray spectrum generator for Monte Carlo simulation tool, developed by the Medical Physics Department, University of Crete in a text file format.[12] These poly-energetic or spectral X-ray beams were created using this tool by setting the input parameters as the target of Tungsten for incident high-energy electrons and a 3.7-mm thick aluminum sheet acting as a filter on the emitting X-ray photons. The dual-energy X-rays considered were 100 kVp and 140 kVp according to the hardware specifications of the HOLOGIC® scanners. The spectra of X-rays of these levels of kVp are demonstrated in Figure 3. The minimum and maximum energies (in keV) were set in the range of 0 to the level of kVp in each case. Likewise, the average X-ray energy for both levels of kVp (100 and 140) were 51.2 and 61.5 keV. To define the source, a histogram with linear interpolation was used for the continuous spectrum of energies. This spectrum in a text file was used as a source in the simulation. An X-ray gun was created to emit unidirectional photons in the direction of the X-axis (traversing the vertebrae and piercing objects). The predefined standard model was used. The cutoff values for electron and photon were considered as 1 cm and 1 mm, respectively. For each of phantoms, two simulations were performed, one using an X-ray at 100-kVp and the other at 140-kVp. For the first phantom (6 cubes with different materials), each simulation was conducted with 100 million particles, and for the second phantom, 300 million particles were used for simulation. The results or outputs were stored in text and root files (using the actors

of the energy spectrum and simulation statistics) as well as planar two-dimensional projections (matrix size: 198 × 280 and pixel size: 1 mm × 1 mm).

Image analysis and plotting

The pair of two-dimensional projections for each phantom were imported into the MATLAB software. In the preprocessing, the projections were rotated, and pixel values were converted to double precision format. Then, in the first phantom, the intensity profile curves for each of the cubes (specified by a particular material) were plotted for 100-kVp and 140-kVp X-ray projections. Subsequently, simple Gaussian smoothing was applied to reduce noise in the images, and then, the resulting smoothed images underwent minimum–maximum normalization (wherein all pixel values fall between 0 and 1). Corresponding images or projections were subtracted pairwise for both phantoms.

Implementation and software

The Monte Carlo particle transport simulation was conducted using the open-source GEANT4-based GATE software (vGate or virtual Gate version 9.0) developed by international openGATE collaboration and installed as a virtual machine under the Linux operating system (version 20.04). For image analysis and curve plotting, MATLAB software (The MathWorks Inc., version 2021b) was utilized. The computer used for the execution of simulations had the following specifications: Intel® Core™ i7-10870H (up to 4.5 GHz, 8 cores, and 16 threads) central processing unit and 32-gigabyte RAM.

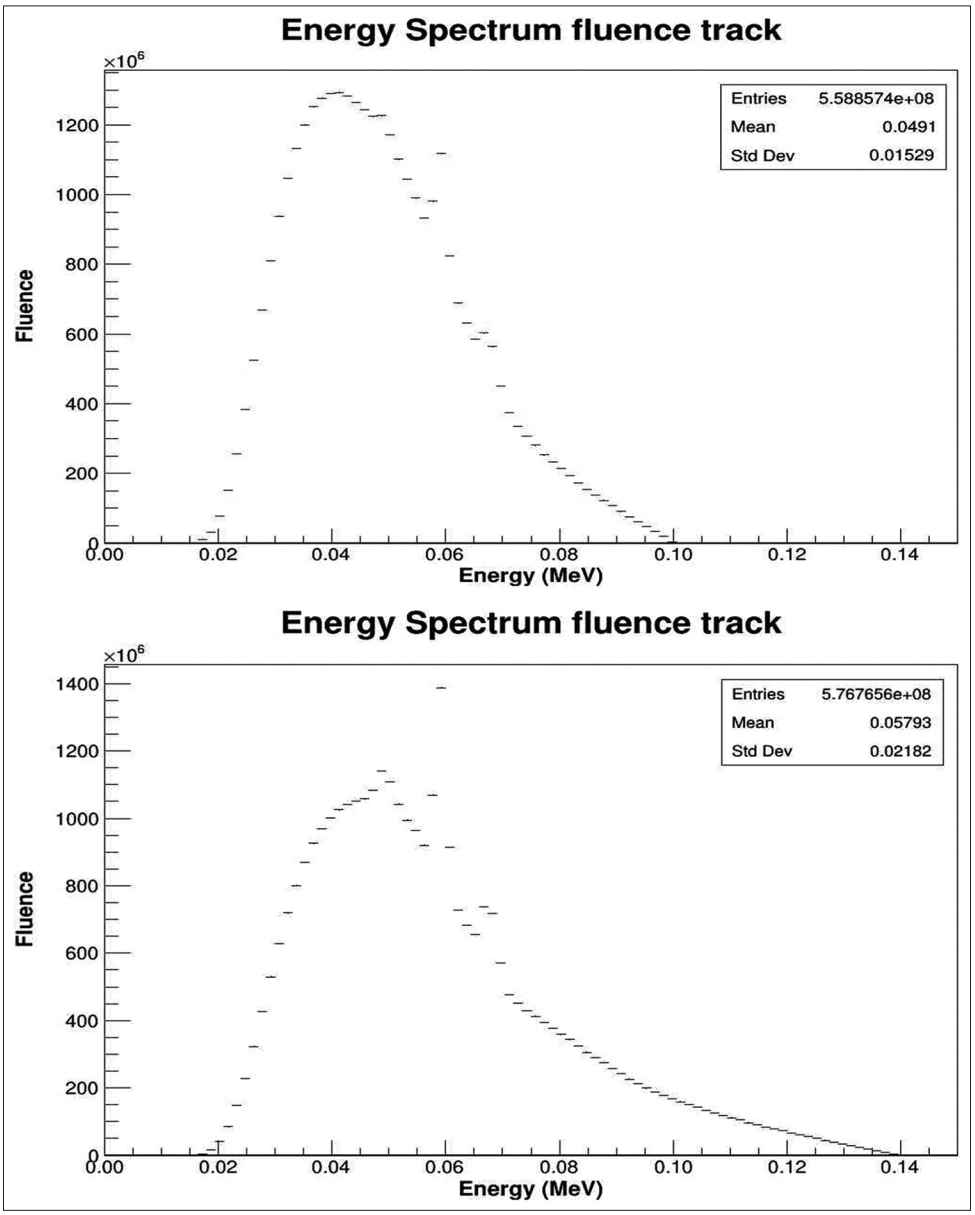

Figure 4: The results of the energy spectrum stored in root files are plotted as histograms for both 100 kVp (upper panel) and 140 kVp (lower panel). Both resemble the energy spectrum generated and simulated

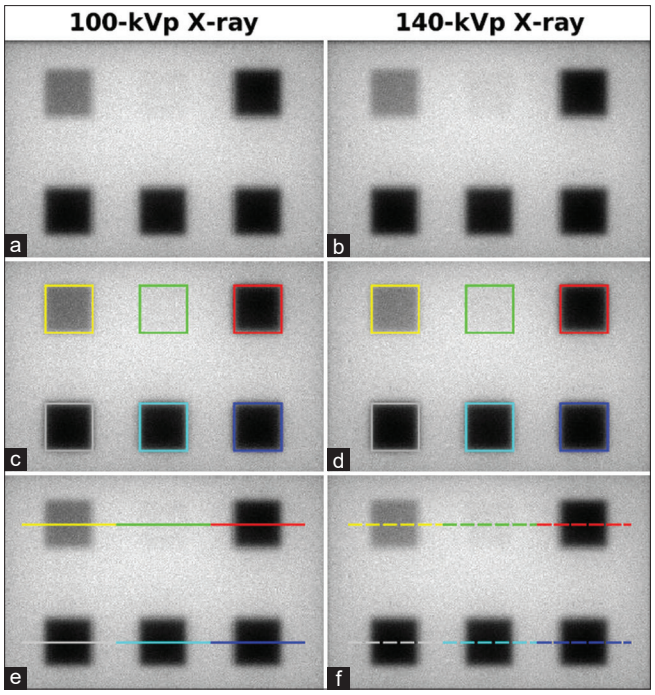

Figure 5: The projections of 100 kVp (a) and 140 kVp, (b) are provided. The squares in the upper and lower rows in each projection or image, (c and d) Correspond to, from left to right, spine bone (yellow box), polymethyl methacrylate (green box), barium sulfate in water (red box), stainless steel alloy (gray box), titanium alloy (cyan box), and gold (blue box). In (e and f), on each box, a line is drawn in the same color to plot the intensity profile curve (solid line for 100 kVp and dashed line for 140 kVp)

Results

As mentioned before, for the first phantom (boxes/cubes), 100 million particles were used which took about 2.5–3 h to complete and for the second phantom (trunk or torso of human body), 300 million particles were generated and the simulation took 4–5 h. The results of energy spectrum fluence stored in root files are plotted as histograms in Figure 4 for both 100 kVp and 140 kVp. Both have similarities to the generated and simulated energy spectra. The projections of 100 and 140 kVp X-rays are displayed [Figure 5a and b, respectively] for the first phantom. The same projections with superimposed rectangles in different colors as mentioned in Figure 2, and lines for profile plotting drawn on each box are demonstrated [Figure 5a-f]. In each projection (of 100 kVp and 140 kVp), the squares in the upper and lower rows correspond to, from left to right, spine bone (yellow box), PMMA (green box), barium sulfate in water (red box), stainless steel alloy (gray box), titanium alloy (cyan box), and gold (blue box). With the exception of the spine bone, where the radio-opacity decreases with increasing X-ray energy (from 100 to 140 kVp), other squares exhibit very imperceptible changes over different energies. PMMA shows consistently very low radio-opacity, whereas others (barium sulfate in water, stainless steel alloy, titanium alloy, and gold) show remarkably high levels of radio-opacity. The background demonstrates the level of radio-opacity for water. In Figure 6, the profile plots of projections for each square are drawn (solid line for 100 kVp and dashed line for 140 kVp) defined by lines drawn in Figure 5e and f. The horizontal line segments

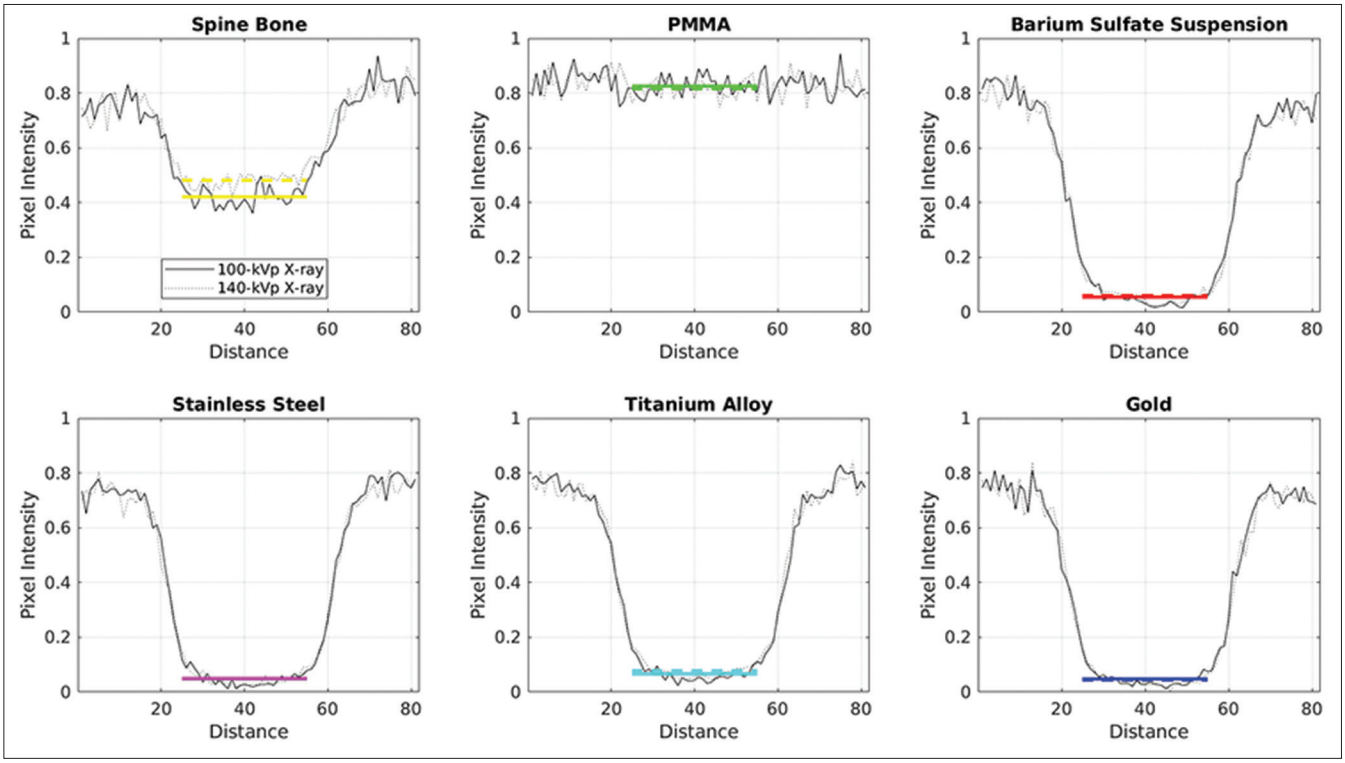

Figure 6: The intensity profile plots of projections for each of 6 cubes or squares are drawn (solid line for 100 kVp and dashed line for 140 kVp) defined by lines drawn in Figure 5e and f across a distance from left to right. PMMA: Polymethyl methacrylate

in the appropriate colors represent the mean intensity value for each box or cube (solid line for 100 kVp and dashed line for 140 kVp). In the spine bone, there is a difference between two horizontal lines. This means that bony structures are clearly visualized against background soft tissue after subtraction of the projections or images. However, in PMMA, X-rays of 100 and 140 kVp are minimally attenuated and no noticeable difference exists among the curves (green solid and dashed horizontal lines). For four other materials (barium sulfate in water, stainless steel alloy, titanium alloy, and gold), all attenuate the X-ray photons substantially in a way that both curves are superimposed at the levels near zero, and thus corresponding horizontal lines are superimposed. Therefore, no perceptible difference is evident among the two curves similar to that for PMMA. Figure 7 displays, similar to that shown in Figure 5, the projections of 100 and 140 kVp X-rays [Figure 7a and b respectively] for the second phantom (body torso or trunk). The silhouettes of vertebrae (L3–L5) are clearly visible but the first vertebra or L1 (composed of PMMA) is hardly noticeable. The transverse colon is significantly dense in all projections. The small round radio-dense regions overlapping the vertebrae (L3–L5) are visualized well-defined indicating the piercing objects. Likewise, the outlines of objects (vertebra, bowel, and piercing items) are drawn with corresponding colors, L1 vertebra in white and other vertebrae in blue, and bowel/colon in magenta, piercing objects in green (stainless steel), gray (titanium), and yellow (gold), in Figure 7c and d. The pairwise subtracted images as those in DXA, are visualized in Figure 8. As can be seen, except for the square of the spine bone, other squares are barely noticeable for all other materials used in this study [Figure 8a and b]. These findings are congruent with those presented as curves in Figure 6. The pairwise subtracted images of the second phantom or body torso are displayed in Figure 8c-e. The small round zones of piercing objects are clearly delineated and are visualized as "holes" in the middle of vertebrae, except for stainless steel piercing objects that is poorly visualized. This pattern is more prominent for piercing objects of gold (on L5 vertebra). Similarly, L1 and also L2 (which is overlapped by transverse colon containing barium sulfate contrast) are not visualized due to the reason for piercing objects.

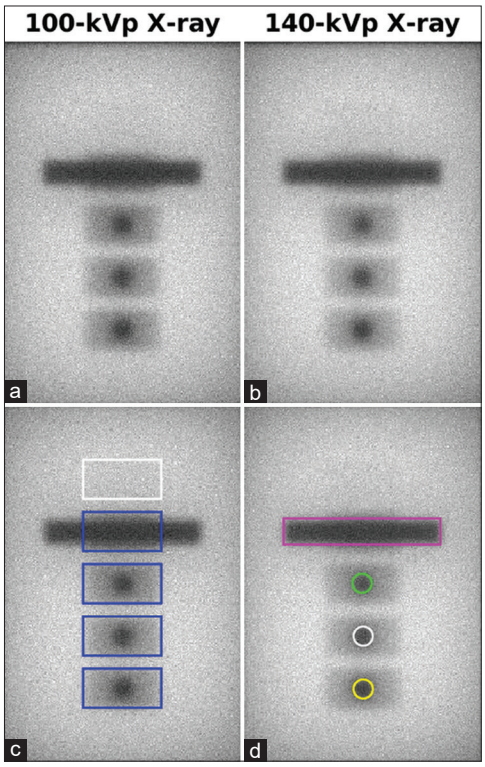

Figure 7: The projections or images of 100 (a) and 140 (b) kVp X-rays are displayed for the second phantom (body torso or trunk). The outlines of vertebrae, bowel, and piercing objects are drawn with their corresponding colors, L1 vertebra in white and other vertebrae in blue, and bowel/colon in magenta, piercing objects in green (stainless steel), gray (titanium), and yellow (gold) are demonstrated (c and d)

Discussion

Artificial high-density materials create artifacts and interfere with BMD measurements and clinical diagnosis. One well-known cause of these artifacts is the prior administration of barium sulfate suspension as a contrast material for medical diagnosis (during contrast-enhanced abdominal computed tomography, barium enema, etc.). Based on the findings of earlier research, the BMD of the lumbar vertebrae that are overlaid by intestinal barium could artifactually increase or even paradoxically decrease, probably as a result of the concentration of barium in the bowels. As previously indicated, to distinguish between bone and soft tissue, the dual-energy X-rays (with kVp of 100 and 140) are utilized in DXA. In the case of the presence of artificial high-density objects or materials, the issue of miscalculation of BMD arises since all X-ray photons with these ranges of energies become nearly equally attenuated, and therefore, no appreciable difference will be present in different projections. This postulate can

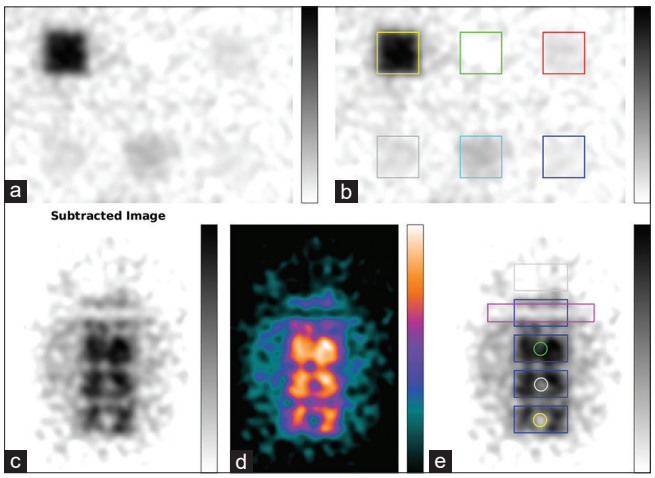

Figure 8: Pairwise subtracted images for the first phantom (a and b) and the second phantom (c-e) displayed in the inverted grayscale and cool color maps. For better clarity, the outlines of boxes or cubes and the vertebrae and piercing objects are demarcated in (b and e), respectively

also be extended to artificial low-density materials. All are eliminated during subtraction of projections as the soft tissues, and as a result, they do not appear in the final image.[6,7] In the present simulation study, we investigated both artificial high- and low-density materials in BMD scanning using HOLOGIC® scanners. The former produces the artifact of black hole and has been evaluated for lead bullets using densitometry scanners or has been documented as incidental findings in other studies.[8,9] But to the best of the knowledge of authors, no evaluation has been carried out for various materials (including steel, gold, etc.) using commercially available densitometry scanners or even as a simulation study. Moreover, the latter and its impact have not been reported or investigated. Hence, we made an effort to simulate the impact of common artificial high- and low-density materials that a practitioner may encounter during their practice. One is barium sulfate, which is a fairly frequent occurrence in hospitalized patients. Another is the piercing items that are commonly used as jewelry by young adults. These objects are predominantly made up of stainless steel alloy or titanium alloys and gold. Finally, apart from these high-density materials, PMMA as a widely used artificial material in orthopedic surgeries (such as vertebroplasty) is investigated as a low-density material in this study. All are compared to the appearance of the spine bone to validate the results. As we found in this study, materials denser than spine bone (1.42 g/cm^3) create profound attenuation on single-energy projections and when subtracted, lead to no perceptible difference in attenuation or absorption. As a result, black-hole artifact appears. The range of densities creating this appearance is enormously wide from 50% suspension of barium sulfate (density higher than 2 g/cm^3) to gold as one the most dense materials (roughly 20 g/cm^3). Stainless steel and titanium alloys are common materials in piercing objects that have densities in this range. Interestingly, PMMA that has a density a little lower than spine bone, near soft tissues or water (1 g/cm^3 or just higher), is assumed to be soft tissue and consequently removed in the final image. These artificial low-density materials also generate the artifact of black hole. In the present study, we used the particular levels of kVp that are applied to X-ray tubes in HOLOGIC® scanners. The presence of this artifact is demonstrated both in clinical and simulated images. There might be differences among vendors, though, and it could be necessary to evaluate this artifact in the scanners of other vendors or manufacturers. Perhaps, validation by these scanners for a wider range of artificial materials is required to provide more convincing evidence.

Conclusion

Denser materials than spine bone create profound attenuation on single-energy projections.The DXA method, which applies subtraction of the projections of two energy spectra, leads to no perceptible difference in attenuation or absorption profiles. As a result, black-hole artifact appears. Interestingly, the range of densities creating this appearance is enormously wide from the density of water to highly dense metallic objects. Stainless steel and titanium alloys are common materials in piercing objects that have densities in this range. PMMA that has a density a little lower than spine bone, near to soft tissues or water (1 g/cm^3 or just higher), is assumed to be soft tissue and consequently removed in the final image. Similar to artificial high-density materials, these artificial low-density materials also generate the artifact of black hole in BMD scans using DEXA method.

Financial support and sponsorship

Nil.

Conflicts of interest

There are no conflicts of interest.

References

1. Albano D, Agnollitto PM, Petrini M, Biacca A, Ulivieri FM, Sconfienza LM, *et al*. Operator-related errors and pitfalls in dual energy X-ray absorptiometry: How to recognize and avoid them. Acad Radiol 2021;28:1272-86.
2. Garg MK, Kharb S. Dual energy X-ray absorptiometry: Pitfalls in measurement and interpretation of bone mineral density. Indian J Endocrinol Metab 2013;17:203-10.
3. Martineau P, Bazarjani S, Zuckier LS. Artifacts and incidental findings encountered on dual-energy X-ray absorptiometry: Atlas and analysis. Semin Nucl Med 2015;45:458-69.
4. Martineau P, Morgan SL, Leslie WD. Bone mineral densitometry reporting: Pearls and pitfalls. Can Assoc Radiol J 2021;72:490-504.
5. Qutbi M, Soltanshahi M, Shiravand Y, Gorzi SK, Shafiei B, Asli IN. Technical and patient-related sources of error and artifacts in bone mineral densitometry using dual-energy X-ray absorptiometry: A pictorial review. Indian J Radiol Imaging 2020;30:362-71.
6. Bonnick SL, Lewis LA. Bone Densitometry for Technologists. 3rd ed. New York: Springer; 2013.
7. International Atomic Energy Agency. Dual Energy X Ray Absorptiometry for Bone Mineral Density and Body Composition Assessment, IAEA Human Health Series No. 15. Vienna: International Atomic Energy Agency; 2011. Available from: https://www-pub.iaea.org/MTCD/Publications/PDF/Corrigenda/p1479_Corrigendum.pdf. [Last accessed on 2023 Dec 17].
8. Morgan SL, Krueger D, Bassler J, Burroughs L, Borchardt G, Yester M, *et al.* Effect of very dense artifacts on Hologic and general electric bone densitometry results. Arch Osteoporos 2020;15:77.
9. Morgan SL, Lopez-Ben R, Nunnally N, Burroughs L, Fineberg N, Tubbs RS, *et al.* Black hole artifacts-a new potential pitfall for DXA accuracy? J Clin Densitom 2008;11:266-75.
10. Azo Materials. Stainless Steel – Grade 316L – Properties, Fabrication and Applications (UNS S31603); 2004. Available from: https://www.azom.com/article.aspx?ArticleID=2382. [Last accessed on 2023 Dec 17].
11. Nuclear Power Titanium Alloys. Available from: https://www.nuclear-power.com/nuclear-engineering/metals-what-are-metals/alloys-composition-properties-of-metal-alloys/titanium-alloys. [Last accessed on 2023 Dec 17].
12. Damilakis J. X-ray Spectrum Generator for Monte Carlo Calculations. University of Crete. Available from: https://ctdose-iqurad.med.uoc.gr/xsg/. [Last accessed on 2024 Jan 17].